Environ. Sci. Technol. 1990, 24, 1848–1856

Kinetics of Selenate and Selenite Adsorption/Desorption at the Goethite/Water Interface

Pengchu Zhang* and Donald L. Sparks

Department of Plant and Soil Sciences, University of Delaware, Newark, Delaware 19717-1303

■ Kinetics and mechanisms of selenate and selenite adsorption/desorption at the goethite/water interface were studied by using pressure-jump (p-jump) relaxation with conductivity detection at 298.15 K. A single relaxation was observed for selenate SeO_4^{2-} adsorption. This relaxation was ascribed to SeO_4^{2-} on a surface site through electrostatic attraction accompanied simultaneously by a protonation process. The intrinsic rate constant for adsorption ($\log k_1^{int} = 8.55$) was much larger than that for desorption ($\log k_{-1}^{int} = 0.52$). The intrinsic equilibrium constant obtained from the kinetic study ($\log K_{kinetic}^{int} = 8.02$) was of the same order of magnitude as that obtained from the equilibrium study ($\log K_{model}^{int} = 8.65$). Unlike SeO_4^{2-}, selenite adsorption on goethite produced two types of complexes, $XHSeO_3^0$ and $XSeO_3^-$, via a ligand-exchange mechanism. Double relaxations were attributed to two reaction steps. The first step was the formation of an outer-sphere surface complex through electrostatic attraction. In the second step, the adsorbed selenite ion replaced a H_2O from the protonated surface hydroxyl group and formed an inner-sphere surface complex. A modified triple layer model (TLM) was employed to describe the adsorption phenomena. The intrinsic equilibrium constants obtained from the equilibrium modeling ($\log K^{int} = 20.42$ for $XHSeO_3^0$ and 15.48 for $XSeO_3^-$) and from the kinetic studies ($\log K^{int} = 19.99$ for $XHSeO_3^0$ and 16.24 for $XSeO_3^-$) were similar, which further verified the hypothesized reaction mechanism.

Introduction

Selenium is important in animal and human nutrition. Although it is not an essential element for plant growth, native vegetation can contain Se levels that are toxic to animals or the vegetation can be deficient in Se, creating animal health difficulties. In fact, there is a very narrow range between deficient and toxic levels of Se in animals, which necessitates a clear knowledge of the processes affecting Se distribution in the environment (*1*, *2*). Recently, concerns have been expressed about Se in the environment. These concerns were brought to the forefront in the 1980s when studies at the Kesterson National Wildlife Refuge in California showed that Se had accumulated in plants and animals at levels that could be deleterious to wildlife. The source of this Se appears to be the subsurface agricultural drainage water from the western San Joaquin Valley that was discharged to Kesterson reservoir to create and manage wetlands. Obviously, the reactions of Se in soil greatly affect the bioaccumulation of Se in plants and animals.

Selenium interactions with soils and soil constituents have focused primarily on selenite retention. In acid soils, Se is immobilized by sesquioxides (*3*). The concentration of selenium in the soil solution was governed primarily by a ferric oxide–selenite adsorption complex, which forms rapidly when selenite is added to soils. However, selenite was also associated with aluminum (*4*) and organic matter in Canadian podzols (*5*). Calcareous soils also retain selenite, but not selenate (*6*). Selenite leaching is increased by addition of SO_4. When the concentration of SO_4 is sufficiently high, it can compete with selenite ions for surface sites (*7*). Studies investigating the pH dependence of selenite adsorption on five alluvial soils suspended in a NaCl background solution showed that selenite adsorption was a function of pH. However, no pH effect on selenite adsorption was observed when SO_4 was present in the suspension (*8*, *9*). Approximately equal competition for adsorption sites between orthophosphate and selenite was observed when both were added at the same initial concentration (2 mmol m^{-3}). These results led Neal et al. (*9*) to hypothesize that selenite and orthophosphate were adsorbed via the same mechanism, viz., ligand exchange (*8*, *9*). This mechanism was previously suggested for the adsorption of selenite on goethite (*10*).

Selenite adsorption on oxides such as gibbsite and goethite appears to be a function of pH (*10–12*). Adsorption vs pH usually reaches a maximum level and the adsorption maximum is insensitive to changes in ionic strength, indicating that the adsorption is not determined by the properties of the diffuse double layer of the outer Helmholtz layer (*11*). Thus, it does not appear that selenite adsorption occurs by electrostatic attraction; rather, a new bond forms between the adsorbed ion and adsorbent.

Hingston et al. (*13*) studied the reversibility of selenite adsorption on goethite and gibbsite. Little of the selenite adsorbed on goethite could be desorbed, whereas selenate adsorption on gibbsite was easily reversible when washed with a 0.1 M NaCl solution at constant pH. The irreversibility observed for selenite adsorption on gibbsite may be due to bridging or multidentate ligand formation and to the formation of ring structures at the surface.

Few reports have appeared in the literature on the adsorption of selenate on soils and soil constituents. Davis and Leckie (*14*) showed that with ionic concentrations of 10^{-5} M the percent of selenate and sulfate adsorbed on amorphous iron oxyhydroxide as a function of pH is essentially the same. Balistrieri and Chao (*12*) and Merrill et al. (*15*) also observed that at the same pH, selenate adsorption on goethite and iron oxyhydroxide is much lower than selenite adsorption. Merrill et al. (*15*) attributed the lower selenate adsorption to competition with sulfate in solution. However, the differences in adsorption of the two selenium species can also be explained by the difference in the affinity of the two oxidation states of selenium for the surface (*12*).

The "mechanisms" that have been proposed for selenate and selenite adsorption on soils and soil constituents have almost totally been based on equilibrium or macroscopic measurements. As Sparks (*16*) has noted, such measurements cannot be used to definitively deduce mechanistic information. Such information can only be derived from spectroscopic and kinetic studies. To obtain direct evidence for the mechanisms of selenite and selenate adsorption on colloidal surfaces, the extended X-ray absorption fine structure (EXAFS) technique was employed to study selenite and selenate interactions with goethite in aqueous suspensions (*17*). Measurements showed that selenate forms a weakly bonded, outer-sphere surface complex and that selenite forms a strongly bonded, inner-sphere complex. The adsorbed selenite ion was directly bonded to the goethite surface in a bidentate fashion

 0013-936X/90/0924-1848$02.50/0

with two Fe atoms 3.38 nm from the selenium atom. Adsorbed selenate had no iron atom in the second coordination shell of selenium, which indicated retention of its hydration sphere upon adsorption (*17*).

Another way to obtain information about mechanisms of selenate and selenite adsorption on soils and soil constituents is to conduct kinetic investigations. Such studies would be especially useful in predicting the rate of retention and release of selenium species in soils. With such information, one could predict the fate of selenium in soils, as it affects surface and groundwater quality and, ultimately, human and animal health.

Unfortunately, the authors are not aware of any studies in the scientific literature on the kinetics of selenium reactions in soils or on soil constituents. This may in part be due to the rapid reactions that are often observed for anion reactions in soils (*16*, *18*). Most traditional kinetic techniques like batch, continuous flow, and stirred flow cannot be used to measure reaction rates with half-times of <30 s. In this study, pressure-jump (p-jump) relaxation was used to determine the mechanisms and kinetics of selenate and selenite adsorption and desorption on goethite, a common soil material that plays an important role in ion retention. The p-jump relaxation technique is based on the principle that chemical equilibrium is dependent on pressure. A sudden change in pressure will alter the equilibrium of a system to a new equilibrium state. The time necessary for the equilibrium adjustment to take place is called the relaxation time (τ), which is related to the rate(s) of the reactions in the system. The p-jump relaxation technique has been used to study the kinetics and mechanisms of adsorption/desorption of cations (*19*, *20*) and anions (*18*, *21*) at the solid/water interface. This technique allows one to measure reactions occurring on millisecond and microsecond time scales.

Materials and Methods

Experimental Procedures. The goethite that was used in this study was prepared according to the procedure described by Atkinson et al. (*22*). It was examined by X-ray diffraction, and the characteristic 0.418-nm peak for goethite was observed. A goethite suspension was dialyzed in deionized water until its conductivity equaled that of fresh deionized water. Then, the suspension was dispersed by using an ultrasonic disperser. The particle size of the dispersed goethite was <2 μm.

Specific surface area of the goethite, which was determined by the ethylene glycol monoethyl ether (EGME) method of Carter et al. (*23*) was 70.1×10^3 m^2 kg^{-1}. A potentiometric titration technique was employed to determine the surface site density of the goethite, which was 6.4 sites nm^{-2}.

The goethite concentration used in the selenate studies was 27.01 g L^{-1}. The original selenate (as Na_2SeO_4) concentration was 3.0×10^{-3} mol L^{-1}, and the ionic strength of the selenate solution, which included the added Na_2SeO_3, NaCl, and HCl, was 1.5×10^{-2} M. In the selenite studies, the goethite concentration was 20.1 g L^{-1}, the initial SeO_3^{2-} concentration was 4.5×10^{-3} mol L^{-1}, and the ionic strength was 2.0×10^{-2} M.

Adsorption isotherms were determined for both selenate and selenite. After a 24-h shaking period, the selenate–goethite and selenite–goethite suspensions were centrifuged at 34500*g* for 30 min. The supernatants were filtered through 0.2-μm-pore membrane filters and the concentrations of selenate and selenite in the filtrate were determined by using a Waters Model 430 ion chromatograph. The pH of the supernatant was also determined.

In the kinetic studies, the relaxation times (τ values) were measured for both selenate– and selenite–goethite suspensions at 0.015 and 0.02 M ionic strengths, respectively, using a Dia-Log p-jump apparatus (Dia-RPC, produced by Dia-Log Co.) and conductivity detector (Dia-RPM, Dia-Log Co.). Before a given selenium–goethite suspension was analyzed kinetically, part of the suspension was separated and pH and selenium concentrations were determined as described previously. During the p-jump relaxation measurement, 13.5 MPa pressure was established on a cell containing the goethite and selenium suspension. Then the pressure was released within 70 μs by bursting a brass membrane of 0.05-mm thickness. A digitizer (Dia-RRC, Dia-Log Co.) was then triggered, and the changes in conductivity of the suspension were caught. The signals were digitized and then sent to a computer. The results of the relaxation could be read from the computer and displayed on an oscilloscope. Detailed information about the p-jump equipment and methods of measurement can be found in Zhang and Sparks (*18*).

Model Application. The modified triple-layer model (TLM) was employed to describe selenate and selenite adsorption on goethite. Theoretical discussions and aspects of the application of the TLM can be found in Hayes and Leckie (*19*). The modified TLM differs from the original model (*14*) in two ways: (i) the adsorbed ion can be located at both the α layer and the β layer rather than only at the β layer; i.e., the adsorbed ion can form an inner- and/or outer-sphere surface complex, not just an outer-sphere complex; and (ii) the chemical potential and standard and reference states are defined equivalently for both solution and surface species, leading to a different relationship between the activity coefficients and the interfacial potential than previously used. The following reactions can be defined for the application of the TLM to selenate and selenite adsorption on goethite using the experimental conditions given earlier:

$$XOH_2^+ \rightleftharpoons XOH + H^+ \quad (1)$$

$$XOH \rightleftharpoons XO^- + H^+ \quad (2)$$

$$XOH_2^+ + Cl^- \rightleftharpoons XOH_2^+ - Cl^- \quad (3)$$

$$XO^- + Na^+ \rightleftharpoons XO^- - Na^+ \quad (4)$$

where XOH is the neutral surface site and XOH_2^+ and XO^- are its protonation and deprotonation forms. For selenate adsorption, it is assumed that the adsorption is nonspecific and the reaction product is an outer-sphere surface complex given as

$$XOH + H^+ + SeO_4^{2-} \rightleftharpoons XOH_2^+ - SeO_4^{2-} \quad (5)$$

If SeO_4^{2-} adsorption is assumed to be specific, viz., a ligand-exchange process occurs, then the reaction can be written as

$$XOH + H^+ + SeO_4^{2-} \rightleftharpoons XSeO_4^- + H_2O \quad (6)$$

For selenite adsorption assuming formation of outer-sphere surface complexes, one can write

$$XOH + 2H^+ + SeO_3^{2-} \rightleftharpoons XOH_2^+ - HSeO_3^- \quad (7)$$

$$XOH + H^+ + SeO_3^{2-} \rightleftharpoons XOH_2^+ - SeO_3^{2-} \quad (8)$$

or, if the adsorption of selenite involves ligand exchange and forms inner-sphere surface complexes then

$$XOH + 2H^+ + SeO_3^{2-} \rightleftharpoons XHSeO_3^0 + H_2O \quad (9)$$

$$XOH + H^+ + SeO_3^{2-} \rightleftharpoons XSeO_3^- + H_2O \quad (10)$$

Table I. Intrinsic Constants for Protonation and Deprotonation and NaCl Adsorption and Desorption on Goethite

$\log K_{a1}^{int}$	−4.3	$\log K_{Na^+}^{int}$	−9.3
$\log K_{a2}^{int}$	−9.8	$\log K_{Cl^-}^{int}$	5.4

where XOH represents 1 mol of reactive surface hydroxyl bound to a Fe ion in goethite. Equations 1 and 2 are the protonation and deprotonation reactions for which their intrinsic equilibrium constants are defined as two acidic constants K_{a1}^{int} and K_{a2}^{int}, respectively. The intrinsic equilibrium constants for the reactions represented in eqs 1–10 are expressed as eqs 11–20:

$$K_{a1}^{int} = \frac{[XOH][H^+]}{[XOH_2^+]} \exp(-F\psi_\alpha/RT) \quad (11)$$

$$K_{a2}^{int} = \frac{[XO^-][H^+]}{[XOH]} \exp(-F\psi_\alpha/RT) \quad (12)$$

$$K_{Cl^-}^{int} = \frac{[XOH_2^+\text{–}Cl^-]}{[XOH_2^+][Cl^-]} \exp(-F\psi_\beta/RT) \quad (13)$$

$$K_{Na^+}^{int} = \frac{[XO^-\text{–}Na^+]}{[XO^-][Na^+]} \exp(F\psi_\beta/RT) \quad (14)$$

$$K_{XOH_2^+\text{–}SeO_4^{2-}}^{int} = \frac{[XOH_2^+\text{–}SeO_4^{2-}]}{[XOH][H^+][SeO_4^{2-}]} \exp(F(\psi_\alpha - 2\psi_\beta)/RT) \quad (15)$$

$$K_{XSeO_4^-}^{int} = \frac{[XSeO_4^-]}{[XOH][H^+][SeO_4^{2-}]} \exp(-F\psi_\alpha/RT) \quad (16)$$

$$K_{XOH_2^+\text{–}HSeO_3^-}^{int} = \frac{[XOH_2^+\text{–}HSeO_3^-]}{[XOH][H^+]^2[SeO_3^{2-}]} \exp(F(\psi_\alpha - \psi_\beta)/RT) \quad (17)$$

$$K_{XOH_2^+\text{–}SeO_3^{2-}}^{int} = \frac{[XOH_2^+\text{–}SeO_3^{2-}]}{[XOH][H^+][SeO_3^{2-}]} \exp(F(\psi_\alpha - 2\psi_\beta)/RT) \quad (18)$$

$$K_{XHSeO_3^0}^{int} = \frac{[XHSeO_3^0]}{[XOH][H^+]^2[SeO_3^{2-}]} \quad (19)$$

$$K_{XSeO_3^-}^{int} = \frac{[XSeO_3^-]}{[XOH][H^+][SeO_3^{2-}]} \exp(-F\psi_\alpha/RT) \quad (20)$$

where F is the Faraday constant, R is the universal gas constant, T is absolute temperature, ψ is the surface potential, and the subscripts α and β indicate the α and β layers, respectively. The intrinsic equilibrium constants for eqs 11–14, obtained from separate potentiometric titration experiments, are given in Table I as well as the two capacitance constants (C_1 and C_2), which are adopted by the TLM to relate surface charge to surface potential. When the adsorption of selenate and selenite on goethite was modeled, the computer program FITEQL (*24*) was used to calculate the intrinsic equilibrium constants for the individual reactions represented in eqs 15–20, the surface charge and potential at each layer, and the exponential terms for each layer. In addition, the FITEQL program is able to compute the species concentrations in the reaction system based on the titration data. The intrinsic constants K_{a1}^{int}, K_{a2}^{int}, $K_{Cl^-}^{int}$, and $K_{Na^+}^{int}$ were fixed when adsorptions of selenite and selenate were modeled.

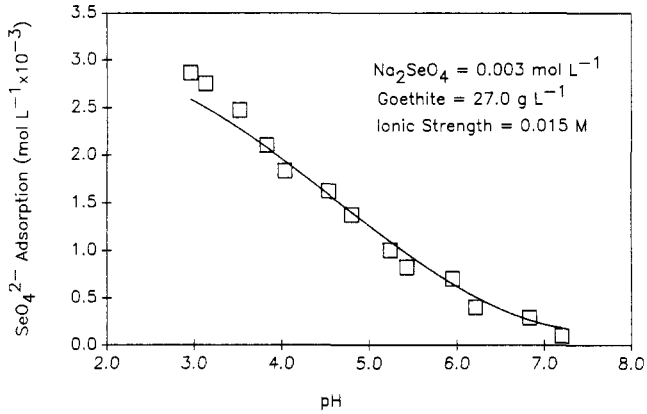

Figure 1. Adsorption of SeO_4^{2-} on goethite vs pH. The symbols represent the experimental data and the solid line represents TLM conformity, assuming nonspecific adsorption with constant C_1 = 1.2 and C_2 = 0.13.

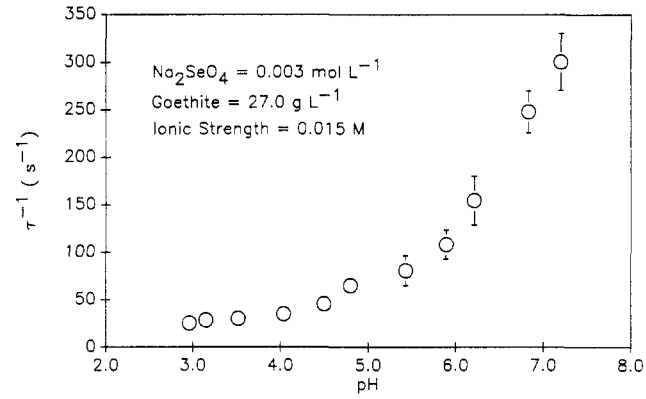

Figure 2. Relationship between pH and reciprocal relaxation times (τ^{-1}) of the selenate–goethite system.

Results and Discussion

Kinetics and Mechanism of Selenate Adsorption on Goethite. Selenate adsorption primarily occurs under acidic conditions, as shown in Figure 1. In the pH range studied, the dominant selenate species is SeO_4^{2-}, since the pK_2 for selenious acid is 2. With an increase in pH, SeO_4^{2-} adsorption rapidly decreased. At pH 2.98, the total percent of adsorption was 93. When pH was higher than 7.2, no adsorption was recorded. Because too much acid was required to reduce the pH lower than 2.98 and to maintain a constant ionic strength of 0.015 M, lower pH experiments were not conducted. Selenate adsorption was described very well by the TLM. With this model, we assumed that the adsorption of SeO_4^{2-} occurs at the β layer via electrostatic attraction to form outer-sphere surface complexes as expressed in eq 5.

Single relaxations were found in selenate–goethite suspensions in the pH range 2.98–7.20. The reciprocal relaxation times (τ^{-1}) increased with an increase in pH or as adsorption decreased (Figure 2). Preliminary experiments involving NaCl–HCl–goethite, NaCl–HCl–goethite supernatant, NaCl–HCl–selenate–goethite supernatant, and NaCl–HCl–Na_2SeO_4 mixed solutions were examined by using p-jump analysis and the same procedure as used for the selenate–goethite system. However, no relaxation was observed. This finding indicates that the relaxation observed for the SeO_4^{2-}–goethite system could be attributed to SeO_4^{2-} adsorption/desorption on the goethite surface. A possible mechanism for SeO_4^{2-} adsorption on goethite, assuming outer-sphere complexation and adsorption of SeO_4^{2-} in the β layer, is that given in eq 5. This mechanism assumes that a SeO_4^{2-} anion adsorbs on a

protonated surface site. The protonation and adsorption of SeO_4^{2-} on the goethite surface occur simultaneously.

For the reaction of SeO_4^{2-} adsorption/desorption at the goethite/water interface expressed in eq 5, the rate is defined as

$$r = -\frac{d[XOH]}{dt} = -\frac{d[SeO_4^{2-}]}{dt} = -\frac{d[H^+]}{dt} = \frac{d[XOH_2^+-SeO_4^{2-}]}{dt} \quad (21)$$

or

$$r = -k_1[XOH][SeO_4^{2-}][H^+] + k_{-1}[XOH_2^+-SeO_4^{2-}] \quad (22)$$

where k_1 and k_{-1} are the rate constants for the forward and backward reactions, respectively, and the terms in the brackets are the time-dependent concentrations. At equilibrium, $r = 0$ and eq 22 becomes

$$0 = -k_1[\overline{XOH}][\overline{SeO_4^{2-}}][\overline{H^+}] + k_{-1}[\overline{XOH_2^+-SeO_4^{2-}}] \quad (23)$$

where the overbar denotes the equilibrium concentration. Relating this to the law of mass action

$$\frac{[\overline{XOH_2^+-SeO_4^{2-}}]}{[\overline{XOH}][\overline{SeO_4^{2-}}][\overline{H^+}]} = \frac{k_1}{k_{-1}} = K' \quad (24)$$

where K' is the conditional equilibrium constant. Following a small perturbation, e.g., a pressure-jump, equilibrium concentrations are shifted a small amount, x. According to the conservation of mass law, the time-dependent concentrations are

$$[XOH] = [\overline{XOH}] + x \qquad [H^+] = [\overline{H^+}] + x$$
$$[SeO_4^{2-}] = [\overline{SeO_4^{2-}}] + x$$
$$[XOH_2^+-SeO_4^{2-}] = [\overline{XOH_2^+-SeO_4^{2-}}] - x$$

Substituting them into eq 22, one obtains

$$r = \frac{dx}{dt} = -k_1([\overline{XOH}] + x)([\overline{SeO_4^{2-}}] + x)([\overline{H^+}] + x) + k_{-1}([\overline{XOH_2^+-SeO_4^{2-}}] - x) = -k_1[\overline{XOH}][\overline{SeO_4^{2-}}][\overline{H^+}] + k_{-1}[\overline{XOH_2^+-SeO_4^{2-}}] - k_1([\overline{XOH}][\overline{SeO_4^{2-}}] + [\overline{XOH}][\overline{H^+}] + [\overline{SeO_4^{2-}}][\overline{H^+}])x - k_1([\overline{XOH}] + [\overline{SeO_4^{2-}}] + [\overline{H^+}])x^2 - k_1x^3 - k_{-1}x \quad (25)$$

The first two terms on the right side of eq 25 vanish because of eq 23. One then obtains

$$\frac{dx}{dt} = -[k_1([\overline{XOH}][\overline{SeO_4^{2-}}] + [\overline{XOH}][\overline{H^+}] + [\overline{SeO_4^{2-}}][\overline{H^+}])]x - k_1([\overline{XOH}] + [\overline{SeO_4^{2-}}] + [\overline{H^+}])x^2 - k_1x^3 \quad (26)$$

which can be further simplified if only small equilibrium perturbations are considered, i.e., small x. Then the last two terms in eq 26 become vanishingly small leading to

$$\frac{dx}{dt} = -[k_1([\overline{XOH}][\overline{SeO_4^{2-}}] + [\overline{XOH}][\overline{H^+}] + [SeO_4^{2-}][\overline{H^+}]) + k_{-1}]x \quad (27)$$

From the definition of relaxation time

$$\frac{dx}{dt} = -\frac{1}{\tau}x \quad (28)$$

Accordingly, the reciprocal relaxation time τ^{-1} can be defined as

$$\tau^{-1} = k_1([XOH][SeO_4^{2-}] + [XOH][H^+] + [\overline{SeO_4^{2-}}][\overline{H^+}]) + k_{-1} \quad (29)$$

Table II. Intrinsic Rate and Equilibrium Constants for SeO_4^{2-} Adsorption and Desorption on Goethite

k_1^{int} mol^{-2} L^2 s^{-1}	3.52×10^8
k_{-1}^{int} s^{-1}	3.34
log $K_{kinetic}^{int}$	8.02
log K_{model}^{int}	8.64

Table III. Relaxation Data for Selenite Adsorption and Desorption on Goethite as a Function of pH at 298 K and an Ionic Strength of 0.02 M

pH	$\tau_{1,obsd}^{-1}$, s^{-1}	$\tau_{1,calcd}^{-1}$, s^{-1}	$\tau_{2,obsd}^{-1}$, s^{-1}	$\tau_{2,calcd}^{-1}$, s^{-1}
6.41	41.6	41.6	9.12	8.54
7.02	46.5	45.1	10.64	9.84
7.50	57.7	58.7	13.62	13.03
7.81	64.1	65.2	14.64	15.21
8.36	79.6	80.3	18.20	19.89
8.73	105.0	105.9	26.19	27.55
9.07	171.5	171.8	29.57	31.68
9.32	249.4	269.7	39.98	42.58
9.64	357.1	357.3	90.50	91.69

The linearized relationship between the reciprocal relaxation time and the concentration of species in suspension for this proposed mechanism is

$$\tau^{-1} = k_1([XOH][SeO_4^{2-}] + [XOH][H^+] + [SeO_4^{2-}][H^+]) + k_{-1} \quad (30)$$

where the terms in the brackets are the concentrations of species at equilibrium. If one considers that the reaction is carried out at the solid/water interface, then the electrostatic effect has to be considered in calculating the intrinsic rate constants. Using the TLM to obtain electrostatic parameters, eq 30 becomes

$$\tau^{-1} = k_1^{int}\exp\left(\frac{-F(\psi_\alpha - 2\psi_\beta)}{2RT}\right)([XOH][SeO_4^{2-}] + [XOH][H^+] + [SeO_4^{2-}][H^+]) + k_{-1}^{int}\exp\left(\frac{F(\psi_\alpha - 2\psi_\beta)}{2RT}\right) \quad (31)$$

In order to obtain a simple first-order equation, eq 31 can be rearranged as

$$\tau^{-1}\exp\left(\frac{-F(\psi_\alpha - 2\psi_\beta)}{2RT}\right) = k_1^{int}\left[\exp\left(\frac{-F(\psi_\alpha - 2\psi_\beta)}{RT}\right) \times ([XOH][SeO_4^{2-}] + [XOH][H^+] + [SeO_4^{2-}][H^+])\right] + k_{-1}^{int} \quad (32)$$

If a plot of the reciprocal relaxation time with the exponential terms on the left-hand side of eq 32 vs the terms in the brackets on the right-hand side of eq 32 results in a linear relationship, then the forward and backward intrinsic rate constants (k_1^{int} and k_{-1}^{int}, respectively), can be determined from the slope and intercept, respectively. It is very clear from Figure 3 that the relationship given in eq 32 is correct. Moreover, computation of the intrinsic equilibrium constant, K^{int}, for the reaction expressed in eq 5 using the kinetic data provides further evidence that the outer-sphere complexation mechanism is correct. In Table II, the intrinsic rate constants, k_1^{int} and k_{-1}^{int}, the intrinsic equilibrium constant from TLM modeling, K_{model}^{int}, and the intrinsic equilibrium constant from the kinetic study, $K_{kinetic}^{int} = k_1^{int}/k_{-1}^{int}$, are presented. On the basis of the agreement between the results from both the equilib-

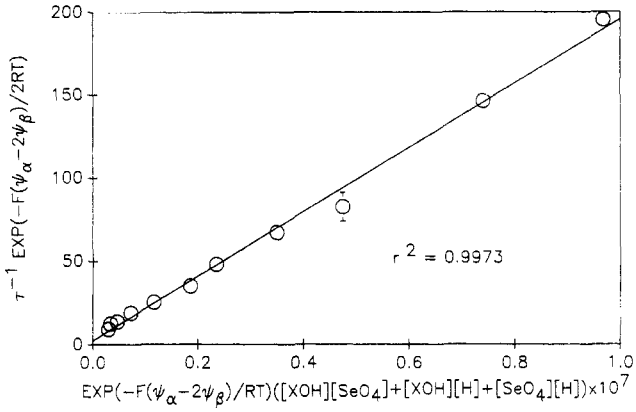

Figure 3. Plot of the relationship between τ^{-1} with exponential and concentration terms as proposed in eq 32.

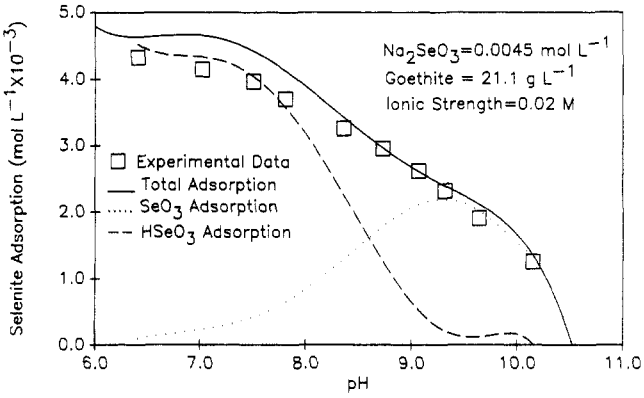

Figure 4. Selenite adsorption vs pH in the selenite–goethite system. The lines represent the prediction of the TLM when inner-sphere surface complex formation is assumed.

rium and the kinetic studies, one can conclude that the assumed reaction mechanism is correct. The same mechanism was found to describe sulfate adsorption on goethite (*21*).

One can also see that the k_1^{int} is 8 orders of magnitude higher than the k_{-1}^{int}, which means that the rate of the adsorption reaction is much higher than the rate of desorption. Therefore, selenate desorption is rate-limiting.

Kinetics and Mechanisms of Selenite Adsorption on Goethite. Total selenite adsorption on goethite decreased with an increase in pH, as illustrated in Figure 4. Data from the modified TLM indicated that, in the pH range studied, selenite adsorbed on the goethite surface to form monovalent and bivalent selenite–Fe complexes, since selenite exists as both SeO_3^{2-} and $HSeO_3^-$ in suspension over the pH range studied. The amounts of both complexes, $XHSeO_3^0$ and $XSeO_3^-$, as shown in Figure 4, are significant in the suspension. This fact implies that neither of them can be ignored nor considered as the dominant species in the suspension. As shown in Figure 4, the amount of $XHSeO_3^0$ dropped sharply at about pH 8.3 (pK_2 = 8.24 for $HSeO_3^-$); meanwhile, the amount of $XSeO_3^-$ increased with pH until pH 8.3 and then dropped as the total adsorption decreased. The solid line in Figure 4 represents the total adsorption as predicted by the TLM; it matches the experimental data very well. Adsorption of $HSeO_3^-$ and SeO_3^{2-} predicted from the TLM are also shown in Figure 4. By use of the FITEQL algorithm, the intrinsic equilibrium constants for the formation of $XHSeO_3^0$ and $XSeO_3^-$, electrostatic parameters such as surface charge and potential at the α and β layers (σ_α, σ_β, ψ_α, and ψ_β), and the concentrations of XOH, XOH_2^+, XO^-, $XHSeO_3^0$, and $XSeO_3^-$ were calculated. It should be

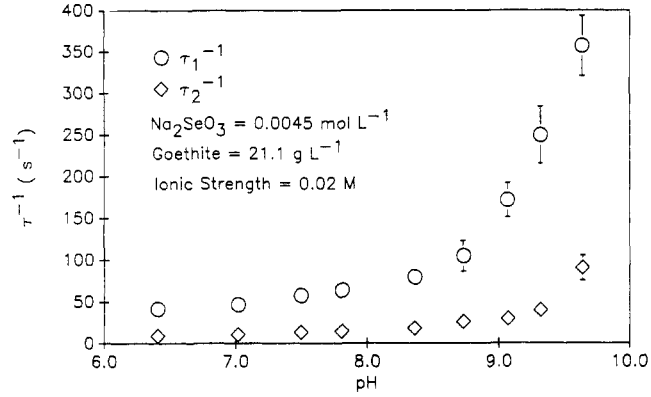

Figure 5. Relationship between pH and fast (τ_1^{-1}) and slow (τ_2^{-1}) reciprocal relaxation times.

pointed out that the intrinsic constants for reactions involving protonation/deprotonation and adsorption of counterion ions are fixed in the FITEQL program, since they are determined from separate potentiometric titration experiments.

The p-jump relaxation studies were carried out over the pH range of 6–10. Double relaxations were observed for the goethite–selenite suspension. Both reciprocal relaxation times, as shown in Figure 5, increased as the pH of the suspensions increased. The procedure for determining the relaxation times from the changes in the amplitude of conductivity vs time after a sudden pressure change is applied can be found in Zhang and Sparks (*18*). In order to ascertain the reactions that caused relaxation, each of the following systems were examined: NaCl–HCl–Na_2SeO_3 mixed solution, Na_2SeO_3–goethite supernatant, NaCl–goethite suspension, and its supernatant. No relaxation(s) was(were) observed with any of these systems. Thus, the relaxations that were observed in the selenite–goethite suspension were caused by adsorption and desorption of selenite on goethite.

On the basis of the findings from the adsorption isotherm and p-jump experiments, one may hypothesize that the mechanism(s) involved in the adsorption and desorption reactions involve(s) the two complexes, $XHSeO_3^0$ and $XSeO_3^-$, and possibly multiple reaction steps. With this in mind, a comprehensive two-step adsorption mechanism was proposed:

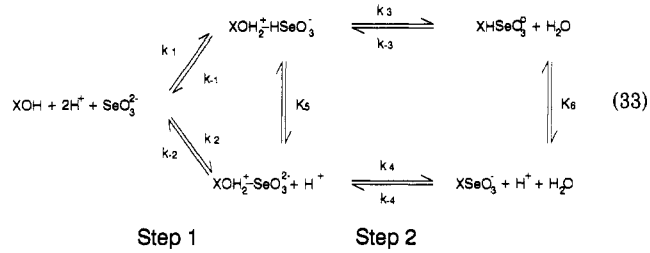

(33)

The first step is the formation of outer-sphere surface complexes (XOH_2^+–$HSeO_3^-$ and XOH_2^+–SeO_3^{2-}) in the β layer. The second step involves a ligand-exchange process, whereby the adsorbed selenite enters the α layer and replaces a ligand from the goethite surface to form the inner-sphere surface complexes ($XHSeO_3^0$ and $XSeO_3^-$). The two protolytic equilibria (represented by K_5 and K_6 and shown by vertical arrows between the complexes in eq 33) are established rapidly compared to the complexation reactions (*25–27*).

To confirm the assumed mechanism in eq 33, one has to (1) derive equations to show the relationships between the reciprocal relaxation times and the concentrations of species involved in the reactions and the rate constants

for each individual elementary reaction; (2) solve the equations so that rate constants can be obtained for the expected mechanism; and (3) use the respective equation, τ_{obsd}^{-1} values, and other concentration terms in the equation to calculate the four unknown intrinsic rate constants (k^{int}) at four of the pH levels studied. These rate constants are then inserted into the rate equation for other pH levels that are studied to calculate τ_{calcd}^{-1} values. If the assumed mechanism is acceptable, the τ_{calcd}^{-1} values will match the τ_{obsd}^{-1} values. Moreover, the intrinsic equilibrium constants for formation of $XHSeO_3^0$ and $XSeO_3^-$ determined from the intrinsic rate constants, which are calculated from the above derived equations ($K_{kinetics}^{int}$), should be consistent with these obtained from equilibrium studies (K_{model}^{int}).

The fast relaxation time, τ_1, observed from the selenite–goethite system, was attributed to step 1 and the slower relaxation, τ_2, to the second step. Two equations relating the τ values to the concentrations of the species in the suspensions should be established to calculate the intrinsic rate constant (k^{int}) for each step in eq 24. Because the derivation processes for the equations are long and tedious, each step will be discussed separately.

Step One. In step one, $HSeO_3^-$, SeO_3^{2-}, and H^+ react with the surface site to form the outer-sphere surface complexes XOH_2^+–$HSeO_3^-$ and XOH_2^+–SeO_3^{2-}, respectively, at the β layer. The conditional equilibrium constants for these reactions are

$$K'_1 = \frac{k_1}{k_{-1}} = \frac{[XOH_2^+\text{–}HSeO_3^-]}{[XOH][H^+]^2[SeO_3^{2-}]} \quad (34)$$

$$K'_2 = \frac{k_2}{k_{-2}} = \frac{[XOH_2^+\text{–}SeO_3^{2-}]}{[XOH][H^+][SeO_3^{2-}]} \quad (35)$$

where the square bracket represents the concentration of species at equilibrium, and k_1, k_{-1}, k_2, and k_{-2} are the rate constants. For simplicity, the following symbols are adopted to represent the concentration terms in eqs 34 and 35.

$$x_1 = [XOH] \qquad x_2 = [XOH_2^+\text{–}HSeO_3^-]$$
$$x_3 = [XOH_2^+\text{–}SeO_3^{2-}] \qquad S = [SeO_3^{2-}] \qquad H = [H^+]$$

The rate law derived for step 1 covering the pH range that was studied is

$$-\frac{dx_1}{dt} = (k_1 + k_2)x_1H^2S - k_{-1}x_2 - k_{-2}x_3H = 0 \quad (36)$$

For a small perturbation caused by a sudden pressure change, there is a small amount of change (Δ) resulting from a deviation in the equilibrium concentration. The rate law then becomes

$$-\frac{d\Delta x_1}{dt} = (k_1 + k_2)(x_1 + \Delta x_1)(H + \Delta H)^2(S - \Delta S) - k_{-1}(x_2 + \Delta x_2) - k_{-2}(x_3 + \Delta x_3)(H + \Delta H) \quad (37)$$

Since the perturbation in the equilibrium of the selenite–goethite system is small, the change in species is very small. All of the terms that contain more than one Δ are deleted because they are extremely small compared with the other terms (*16*, *28*). Equation 37 can now be written as

$$-\frac{d\Delta x_1}{dt} = (k_1 + k_2)(x_1H^2S) - k_{-1}x_2 - k_{-2}(x_3H) + (k_1 + k_2)(2x_1HS\Delta H + H^2S\Delta x_1 + x_1H^2\Delta S) - k_{-1}\Delta x_2 - k_{-2}(H\Delta x_3 + x_3\Delta H) \quad (38)$$

According to eq 36, the first three terms in eq 38 can be canceled, and thus eq 38 becomes

$$-\frac{d\Delta x_1}{dt} = (k_1 + k_2)(2x_1HS\Delta H + H^2S\Delta x_1 + x_1H^2\Delta S) - k_{-1}\Delta x_2 - k_{-2}(H\Delta x_3 + x_3\Delta H) \quad (39)$$

The definition for relaxation time is

$$-\frac{d\Delta x}{dt} = \frac{1}{\tau}\Delta x \quad (40)$$

Accordingly, the reciprocal relaxation time, τ_1^{-1}, can be defined as

$$\tau_1^{-1} = (k_1 + k_2)\left(2x_1HS\frac{\Delta H}{\Delta x_1} + H^2S\frac{\Delta x_1}{\Delta x_1} + x_1H^2\frac{\Delta S}{\Delta x_1}\right) - k_{-1}\frac{\Delta x_2}{\Delta x_1} - k_{-2}\left(H\frac{\Delta x_3}{\Delta x_1} + x_3\frac{\Delta H}{\Delta x_1}\right) \quad (41)$$

The task now is to substitute the terms with Δ in eq 41 with the equilibrium concentrations since the changes in concentration cannot be determined directly. From mass balance

$$\Delta x_1 + \Delta x_2 + \Delta x_3 = 0 \qquad \Delta x_1 = \Delta S$$

and eqs 34 and 35, one can derive the equations

$$\frac{\Delta x_2}{x_2} = \frac{\Delta x_1}{x_1} + \frac{\Delta S}{S} + \frac{2\Delta H}{H} \quad (42)$$

$$\frac{\Delta x_3}{x_3} = \frac{\Delta x_1}{x_1} + \frac{\Delta S}{S} + \frac{\Delta H}{H} \quad (43)$$

The program MACSYMA (*29*) was used to establish a complete relationship between the reciprocal relaxation time and the equilibrium concentrations and the rate constants. Since XOH_2^+–$HSeO_3^-$ and XOH_2^+–SeO_3^{2-} are the intermediate products and their concentrations cannot be determined directly, only the concentrations of reactants are used in the rate equation. The final equation in which the reciprocal relaxation time is a function of equilibrium concentrations of XOH, SeO_3^{2-}, and H^+ and the rate constants k_1, k_2, k_{-1}, and k_{-2} instead of a function of Δs is

$$\tau_1^{-1} = (k_1 + k_2)\left[H^2(x_1 + S) - \frac{2H[(H^2k_1k_{-2} + Hk_2k_{-1})(x_1 + S) + k_{-1}k_{-2}]}{(2Hk_1k_{-2} + k_2k_{-1})S}\right] - k_{-2}\left[\frac{H[H^2k_1k_2(x_1 + 1) - k_2k_{-1}]}{2Hk_1k_{-2} + k_2k_{-1}} - \frac{(H^2k_1k_{-2} + Hk_2k_{-1})(x_1 + S) + k_{-1}k_{-2}}{(2Hk_1k_{-2} + k_2k_{-1})S}\right] + k_{-1}\left[\frac{H^2k_1k_2(x_1 + 1) - k_2k_{-1}}{2Hk_1k_{-2} + k_2k_{-1}} + 1\right] \quad (44)$$

Since the selenite reactions are carried out at the solid/water interface, the effects of the charged surface have to be considered. The intrinsic equilibrium constants and rate constants can be related to the conditional constants as follows:

$$K_1^{int} = \frac{[XOH_2^+\text{–}HSeO_3^-]}{[XOH][H^+]^2[SeO_3^{2-}]}\exp\left(\frac{F(\psi_\alpha - \psi_\beta)}{RT}\right) = K'_1\exp\left(\frac{F(\psi_\alpha - \psi_\beta)}{RT}\right) \quad (45)$$

$$K_2^{int} = \frac{[XOH_2^+\text{-}SeO_3^{2-}]}{[XOH][H^+][SeO_3^{2-}]} \exp\left(\frac{F(\psi_\alpha - 2\psi_\beta)}{RT}\right) = K'_2 \exp\left(\frac{F(\psi_\alpha - 2\psi_\beta)}{RT}\right) \quad (46)$$

Relating these to the rate constants, one obtains

$$K'_1 = \frac{k_1}{k_{-1}} = \frac{k_1^{int}}{k_{-1}^{int}} \exp\left(\frac{-F(\psi_\alpha - \psi_\beta)}{RT}\right) = \frac{k_1^{int} \exp\left(\frac{-F(\psi_\alpha - \psi_\beta)}{2RT}\right)}{k_{-1}^{int} \exp\left(\frac{F(\psi_\alpha - \psi_\beta)}{2RT}\right)} \quad (47)$$

$$K'_2 = \frac{k_2}{k_{-2}} = \frac{k_2^{int}}{k_{-2}^{int}} \exp\left(\frac{-F(\psi_\alpha - 2\psi_\beta)}{RT}\right) = \frac{k_2^{int} \exp\left(\frac{-F(\psi_\alpha - 2\psi_\alpha)}{2RT}\right)}{k_{-2}^{int} \exp\left(\frac{F(\psi_\alpha - 2\psi_\alpha)}{2RT}\right)} \quad (48)$$

In eq 44, all of the rate constants (k) will be substituted by the intrinsic rate constants (k^{int}) and their exponential terms and the final solutions are obtained by solving four simultaneous equations. The computer program NAG Fortran Library, Mark II (*30*), was employed to solve the equations. The exponential terms were calculated from the results of the TLM at the pH levels that were studied. To obtain the correct and accurate solution for a specific case, one must (1) choose a reasonable range for each k^{int} and (2) minimize the allowed error in the computer program, since the constants in the equations vary from 10^2 to 10^{-20}. Double precision was adopted in the program that was employed and the estimated values for the k^{int} values were very slowly increased or decreased during the looping procedure. The intrinsic rate constants (k_1^{int}, k_{-1}^{int}, k_2^{int}, and k_{-2}^{int}) for the first step of the selenite–goethite reaction mechanism are listed in Tables IV and V.

To examine the plausibility of the mechanism in eq 33, the similarility in results from the thermodynamic and kinetic studies must be compared. This involves two tests: (1) inserting the values of τ_1^{-1}, and the concentration and electrostatic parameters at the four pH levels that were studied into eq 44 to calculate intrinsic rate constants k^{int} and then (2) by inserting the concentration and electrostatic parameters at the other pH levels into eq 44 in which the k^{int} were now known, one could determine the values of $\tau_{1,calcd}^{-1}$. If the intrinsic rate constants (k^{int}) were correct, then (1) the values of $\tau_{1,calcd}^{-1}$ would agree with the experimental values of the reciprocal relaxation times ($\tau_{1,obsd}^{-1}$) at each pH level that was studied, and (2) the overall intrinsic constants for the reactions of formation of $XHSeO_3^0$ and $XSeO_3^-$ should be of the same order of magnitude. Table III lists the fast reciprocal relaxation times (τ_1^{-1}) obtained experimentally ($\tau_{1,obsd}^{-1}$) and those calculated from eq 44 at the various pH values that were studied ($\tau_{1,calcd}^{-1}$). One can see that these values are quite similar.

Step Two. In this step, divalent and monovalent selenite anions enter the α layer to replace a molecule of water from the active site and form inner-sphere surface complexes, $XSeO_3^-$ and $XHSeO_3^0$, respectively. The following

Table IV. Intrinsic Rate Constants and Equilibrium Constants for $HSeO_3^-$ Adsorption and Desorption on Goethite

	k_1^{int}, $mol^{-3}\ L^3\ s^{-1}$	k_{-1}^{int}, s^{-1}	k_3^{int}, s^{-1}	k_{-3}^{int}, s^{-1}	log $K_{XHSeO_3}^{int}$
equilibrium study					20.42
kinetic study	3.82×10^{14}	4.07	101.0	9.7×10^{-5}	19.99

Table V. Intrinsic Rate Constants and Equilibrium Constants for SeO_3^{2-} Adsorption and Desorption on Goethite

	k_2^{int}, $mol^{-2}\ L^2\ s^{-1}$	k_{-2}^{int}, s^{-1}	k_4^{int}, s^{-1}	k_{-4}^{int}, s^{-1}	log $K_{XSeO_3}^{int}$
equilibrium study					15.48
kinetic study	2.18×10^{13}	3.26×10^{-3}	0.13	0.05	16.24

nomenclature is adopted to simplify the terms in the equation derivation, $x_4 = [XSeO_3^-]$ and $x_5 = [XHSeO_3^0]$. In the second step the rate law for the change in concentration of the species after a small perturbation is

$$-\frac{d(\Delta x_2 + \Delta x_3)}{dt} = k_3\Delta x_2 - k_{-3}\Delta x_5 + k_4\Delta x_3 - k_{-4}\Delta x_4 \quad (49)$$

The reciprocal relaxation time is expressed as

$$\tau_2^{-1} = \frac{k_3}{1 + \frac{\Delta x_3}{\Delta x_2}} + \frac{k_{-3}}{1 + \frac{\Delta x_4}{\Delta x_5}} + \frac{k_4}{1 + \frac{\Delta x_2}{\Delta x_3}} + \frac{k_{-4}}{1 + \frac{\Delta x_5}{\Delta x_4}} \quad (50)$$

From the mass balance existing in step 2

$$\Delta x_2 + \Delta x_3 + \Delta x_4 + \Delta x_5 = 0 \quad (51)$$

$$\Delta x_2 + \Delta x_5 + \Delta H = 0 \quad (52)$$

and the relationships

$$K_5 = \frac{x_3 H}{x_2} \qquad K_6 = \frac{x_4 H}{x_5}$$

two equations result

$$\frac{\Delta x_3}{x_3} + \frac{\Delta H}{H} - \frac{\Delta x_2}{x_2} = 0 \quad (53)$$

$$\frac{\Delta x_4}{x_4} + \frac{\Delta H}{H} - \frac{\Delta x_5}{x_5} = 0 \quad (54)$$

As was mentioned before, $XOH_2^+\text{-}HSeO_3^-$ and $XOH_2^+\text{-}SeO_3^{2-}$ are the intermediate products and their concentrations cannot be directly determined. Therefore, it is necessary to express the relaxation times as a function of the concentrations of the final products, $XHSeO_3^0$ and $XSeO_3^-$. Accordingly, the relationship between τ_2^{-1} and $XHSeO_3^0$ and $XSeO_3^-$ was obtained with the program MACSYMA:

$$\tau^{-1}{}_2 = k_{-3}/\left[\frac{(f_7k_{-3} + f_4k_3)k_{-4} + f_5k_{-3}k_4}{(f_1k_{-3} + f_5k_3)k_{-4} + f_6k_{-3}k_4} + 1\right] + k_{-4}/\left[\frac{(f_1k_{-3} + f_5k_3)k_{-4} + f_6k_{-3}k_4}{(f_7k_{-3} + f_4k_3)k_{-4} + f_5k_{-3}k_4} + 1\right] + k_4/\left[\frac{f_1k_{-3}k_{-4} + f_2k_{-3}k_4}{(f_7k_{-3} + f_3k_3)k_{-4}} + 1\right] + k_3/\left[\frac{(f_7k_{-3} + f_3k_3)k_{-4}}{f_1k_{-3}k_{-4} + f_2k_{-3}k_4} + 1\right] \quad (55)$$

where

$$f_1 = x_4x_5^2 \qquad f_2 = (x_5^2 + x_4x_5)H + x_4x_5^2$$
$$f_3 = (x_4x_5 + x_4^2)H + x_4^2x_5 \qquad f_4 = x_4^2(H + x_5)$$
$$f_5 - x_4x_5H \qquad f_6 = x_5^2(H + x_4) \qquad f_7 = x_4^2x_5$$

As for the final equation in step 2, the rate constants (k) in eq 55 are expressed as their intrinsic forms (k^{int}) and the exponential terms indicate the effect of the electric double layer. The relationships between the intrinsic equilibrium constants (K^{int}) and the conditional equilibrium constants (K') are

$$K_3^{int} = \frac{[XHSeO_3^0]}{[XOH_2^+\text{-}HSeO_3^-]} \exp\left(\frac{-F(\psi_\alpha - \psi_\beta)}{RT}\right) = K'_3 \exp\left(\frac{-F(\psi_\alpha - \psi_\beta)}{RT}\right) \quad (56)$$

$$K_4^{int} = \frac{[XSeO_3^-] \exp\left(\frac{-F\psi_\alpha}{RT}\right)}{[XOH_2^+\text{-}SeO_3^{2-}] \exp\left(\frac{F(\psi_\alpha - 2\psi_\beta)}{RT}\right)} = K'_4 \exp\left(\frac{-2F(\psi_\alpha - \psi_\beta)}{RT}\right) \quad (57)$$

Correspondingly, the intrinsic rate constants and the intrinsic equilibrium constants have the relationships

$$K_3^{int} \exp\left(\frac{F(\psi_\alpha - \psi_\beta)}{RT}\right) = \frac{k_3^{int} \exp\left(\frac{F(\psi_\alpha - \psi_\beta)}{2RT}\right)}{k_{-3}^{int} \exp\left(\frac{-F(\psi_\alpha - \psi_\beta)}{2RT}\right)} \quad (58)$$

$$K_4^{int} \exp\left(\frac{2F(\psi_\alpha - \psi_\beta)}{RT}\right) = \frac{k_4^{int} \exp\left(\frac{F(\psi_\alpha - \psi_\beta)}{RT}\right)}{k_{-4}^{int} \exp\left(\frac{-F(\psi_a - \psi_\beta)}{RT}\right)} \quad (59)$$

Substituting the exponential terms in eq 58 and eq 59 into eq 55, one obtains a long nonlinear equation. Again, the NAG program is employed to solve four simultaneous equations so as to obtain the four k^{int} values in the nonlinear equation with the addition of exponential terms. The solutions are given in Tables IV and V. As was done for the first reaction step, the k^{int} values were used in eq 55 to calculate the other τ_2^{-1} values at which the p-jump experiment was conducted. The results, $\tau_{2,obsd}^{-1}$ and $\tau_{2,calcd}^{-1}$, are listed in Table III, and they are in close agreement, indicating that the mechanism hypothesized for step 2 in eq 33 is correct.

Summary. The data listed in Table III show values of reciprocal relaxation times obtained by both experimentation and calculation at the pH levels that were studied. They agree with each other very well. This finding indicates that the intrinsic rate constants for each reaction in the two-step reaction scheme are acceptable. Thus, the assumed reaction mechanism is verified kinetically. Moreover, the intrinsic equilibrium constants can be obtained from the rate constants by using the following equations:

$$K^{int}_{XHSeO_3^0} = \frac{k_1^{int}}{k_{-1}^{int}} \frac{k_3^{int}}{k_{-3}^{int}} \quad (60)$$

$$K^{int}_{XSeO_3^-} = \frac{k_2^{int}}{k_{-2}^{int}} \frac{k_4^{int}}{k_{-4}^{int}} \quad (61)$$

As shown in Tables IV and V, the intrinsic equilibrium constants determined from the equilibrium study and the kinetic study are of the same order of magnitude. This provides further evidence that the assumed reaction mechanism is verified.

In summary, adsorption of selenite on goethite produces two types of complexes: the protonated selenite anion ($HSeO_3^-$) with the active site on the goethite surface, and the bivalent selenite anion (SeO_3^{2-}) reacting with the surface site. The proportion of each complex depends on the pH of the suspension. Both of these are inner-sphere surface complexes. The formation of the inner-sphere surface complexes involves two steps: selenite first forms an outer-sphere surface complex at the β layer, and then a ligand is replaced from the surface site by either adsorbed $HSeO_3^-$ or SeO_3^{2-}. The adsorbed selenite binds directly to the surface site to form an inner-sphere surface complex. The second step is much slower than the first step and thus is rate-limiting.

Registry No. SeO_3^{2-}, 14124-67-5; $HSeO_3^-$, 20638-10-2; SeO_4, 14124-68-6; Na^+, 7440-23-5; Cl^-, 16887-00-6; geothite, 1310-14-1.

Literature Cited

(1) Jacobs, L. S. *Selenium in Agriculture and the Environment*; *SSSA Spec. Publ.* **1989**, *No. 23*.
(2) McNeal, I. M.; Balistrieri, L. S. In *Selenium in Agriculture and the Environment*; Jacobs, L. S., Ed.; *SSSA Spec. Publ.* **1989**, *No. 23*, 1–13.
(3) Cary, E. E.; Wiecaonek, G. A.; Allaway, W. H. *Soil Sci. Soc. Am. Proc.* **1967**, *31*, 21–26.
(4) Geering, H, R.; Cary, E. E.; Johnes, L. P.; Llarvay, W. H. *Soil Sci. Soc. Am. Proc.* **1968**, *32*, 35–40.
(5) Levewque, M. *Can. J. Soil Sci.* **1974**, *54*, 63–68.
(6) Johns, G. B.; Belling, G. B. *Aust. J. Agric. Res.* **1967**, *18*, 733–740.
(7) Brown, M. J.; Carter, D. L. *Soil Sci. Soc. Am. Proc.* **1969**, *33*, 563–565.
(8) Neal, R. H.; Sposito, G.; Holtzclaw, K. M.; Traina, S. J. *Soil Sci. Soc. Am. J.* **1987**, *51*, 1161–1165.
(9) Neal, R. H.; Sposito, G.; Holtzclaw, K. M.; Traina, S. J. *Soil Sci. Soc. Am. J.* **1987**, *51*, 1165–1169.
(10) Hingston, F. J.; Posner, A. M.; Quirk, J. P. *Discuss. Faraday Soc.* **1971**, *52*, 334–342.
(11) Hingston, F. J.; Atkinson, R. J.; Posner, A. M. *Nature* **1971**, *215*, 1459–1461.
(12) Balistrieri, L. S.; Chao, T. T. *Soil Sci. Soc. Am. J.* **1987**, *51*, 1145–1151.
(13) Hingston, F. J.; Posner, A. M.; Quirk, J. P. *J. Soil Sci.* **1974**, *25*, 16–26.
(14) Davis, J. A.; Leckie, J. O. *J. Colloid. Interface Sci.* **1980**, *74*, 32–43.
(15) Merrill, D. T.; Manzione, M. A.; Peterson, J. J.; Parker, D. S.; Chow, W.; Hobbs, A. O. *J.—Water Pollut. Control Fed.* **1986**, *58*, 18–26.
(16) Sparks, D. L. *Kinetics of Soil Chemical Processes*; Academic Press: New York, 1989; Chapter 4.
(17) Hayes, K. F.; Roe, H. L.; Brown, G. E.; Hodgson, K. O.; Leckie, J. O.; Parks, G. A. *Science* **1987**, *238*, 783–786.
(18) Zhang, P.; Sparks, D. L. *Soil Sci. Soc. Am. J.* **1989**, *53*, 1028–1034.
(19) Hayes, K. F.; Leckie, J. O. In *Geochemical Processes at Mineral Surfaces*; Davis, J. A., Hayes, K. F., Eds.; ACS Symposium Series 323; American Chemical Society: Washington, DC, 1987.
(20) Hachiya, K.; Ashida, M.; Sasaki, M.; Karasuda, M.; Yasunaga, T. *J. Phys. Chem.* **1980**, *84*, 2292–2296.

(21) Zhang, P.; Sparks, D. L. *Soil Sci. Soc. Am. J.*, in press.
(22) Atkinson, R. J.; Posner, A. M.; Quirk, J. P. *J. Phys. Chem.* **1967**, *71*, 550-558.
(23) Carter, D. L.; Mortland, M. M.; Kemper, W. D. In *Methods of Soil Analysis*, 2nd ed.; Klute, A., Ed.; Soil Science Society of America: Madison, WI, 1986; Part I, pp 413-423.
(24) Westall, J. C. FITEQL; Oregon State University: Corvallis, OR, 1982.
(25) Eigen, M.; De Maeyer, L. In *Techniques in Organic Chemistry*, 2nd ed.; Weissberger, A., Ed.; Wiley Interscience: New York, 1963; Vol. 8, Part 2.
(26) Patel, R. C.; Taylor, R. S. *J. Phys. Chem.* **1973**, *77*, 2318-2323.
(27) Patel, R. C.; Atkinson, G.; Boe, R. J. *Chem. Instrum. (N.Y.)* **1974**, *5*, 243-255.
(28) Bernasconi, C. F. *Relaxation Kinetics*; Academic Press: New York, 1976; Chapter 1.
(29) Rand, R. H. *Computer Algebra in Applied Mathematics: An Introduction to MACSYMA*; Pitman Advanced Publishing Program, London, 1984.
(30) NAG Fortran Library Manual Mark II; Numerical Algorithms Group Ltd., Downers Grove, IL, 1984.

Received for review April 19, 1990. Revised manuscript received July 16, 1990. Accepted July 24, 1990.

Choosing between High-Resolution Mass Spectrometry and Mass Spectrometry/Mass Spectrometry: Environmental Applications

M. Judith Charles*

Department of Environmental Sciences and Engineering, University of North Carolina at Chapel Hill, Chapel Hill, North Carolina 27599-7400

Yves Tondeur

Triangle Laboratories, Inc., 801-10 Capitola Drive, P.O. Box 13485, Research Triangle Park, North Carolina 27709

■ Selectivity in environmental analyses requires the use of fractionation techniques and HRMS or MS/MS to eliminate specific and nonspecific interferences. In the analysis of TCDDs and TCDFs, HRMS is the method of choice when specific interferences arising from compounds with molecular or fragment ions can be separated from TCDD and TCDF ions at a resolving power of 10000. In cases where HRMS does not provide adequate selectivity at this resolving power, MS/MS is needed. Analyses on a pulp and paper effluent extract show that MS/MS was able to substantially eliminate interferences due to the presence of methyl and ethyl tetrachlorinated dibenzofurans that were not removed by HRMS at resolving powers of 10000 and 18000. Nonspecific interferences may also be present due to coelution of compounds that cause changes in the response of the mass spectrometer and are best eliminated by fractionation techniques or by altering conditions of analyses.

Introduction

Questions and problems that an analyst encounters in choosing between high-resolution mass spectrometry (HRMS) and mass spectrometry/mass spectrometry (MS/MS) are exemplified in the analysis of tetrachlorinated dibenzo-*p*-dioxins (TCDDs) and tetrachlorinated dibenzofurans (TCDFs). TCDDs and TCDFs exist in environmental matrices as components of complex mixtures at trace levels (ppt, ppq) compared to the other environmental contaminants. Detection and quantification at these low levels require sensitivity and selectivity. Selectivity is achieved by fractionation techniques in combination with high-resolution gas chromatography and HRMS or MS/MS.

Fractionation procedures using acid/base-treated silica gel, alumina, and carbon columns separate polychorinated dibenzo-*p*-dioxins (PCDDs) and polychlorinated dibenzofurans (PCDFs) from the bulk material (*1*), leaving behind coextractables that can act as specific and nonspecific interferences (*2*). These interferences affect instrument sensitivity and stability (*1*, *2*).

Specific interferences are due to compounds remaining in sample extracts that exhibit molecular or fragment ions that are not resolved from ions monitored for TCDDs and TCDFs at low-resolution MS. These interferences lead to either false positive or negative results. They can be alleviated by optimization of sample fractionation techniques and/or use of HRMS or MS/MS. Examples of specific interferences that can be eliminated by HRMS at a resolving power of 10000 by selected ion monitoring (SIM) techniques, where ions of a given elemental composition are measured (*2*, *3*), are nonachlorobiphenyl, DDE, tetrachlorinated methoxybiphenyl, and tetrachlorinated benzyl phenyl ether (*2*). Pentachlorinated benzyl phenyl ethers, tetrachlorinated xanthenes, and tetrachlorinated methyl- and ethyldibenzofurans are specific interferences that require HRMS analysis at resolving powers greater than 18000 (*3*, *9*). The presence of polychorinated biphenyls (PCBs) is exacerbated if M - COCl confirming ions of TCDD are monitored. Interferences in M - COCl channels due to the loss of three chlorines from hexachlorobiphenyl and four chlorines from heptachlorobiphenyl require resolving powers on the order of 300000 and 48000, respectively (*2*, *3*). Enhanced selectivity needed to separate these ions from TCDD ions requires the use of MS/MS by selected reaction monitoring (SRM), where the parent ion is transmitted through the first mass analyzer (MS1) to a collision cell area and collisionally induced daughter ions characteristic to the analyte of interest are formed and detected on a second mass analyzer (MS2) (*5*). Since daughter ion formation is affected by the collision energy, nature of the collision gas, and collision gas pressure, optimization of an MS/MS method requires considering the effect of these parameters on collision-induced dissociations (CID) of the analyte.

Nonspecific interferences originate from substances generally of unknown composition and structure that remain after sample cleanup. These interferences coelute within the TCDD/TCDF GC retention time window and result in changes on measurement and detection of TCDDs and TCDFs.

In this study, we present results of experiments conducted to optimize MS/MS for the analysis of PCDDs and PCDFs and examples of how specific and nonspecific interferences affect identification and quantification of

 0013-936X/90/0924-1856$02.50/0